Dynamics of cell type transition mediated by epigenetic modifications

Rongsheng Huang[a], Qiaojun Situ[b], Jinzhi Lei[c,*]

[a]*School of Science, Jimei University, Xiamen Fujian 361021, China*
[b]*Zhou Pei-Yuan Center for Applied Mathematics, Tsinghua University, Beijing 100084, China*
[c]*School of Mathematical Sciences, Center for Applied Mathematics, Tiangong University, Tianjin, 300387, China*

Abstract

Maintaining tissue homeostasis requires proper regulation of stem cell differentiation. The Waddington landscape suggests that gene circuits in a cell form a potential landscape of different cell types, with cells developing into different cell types following attractors of the probability landscape. However, it remains unclear how adult stem cells balance the trade-off between self-renewal and differentiation. We propose that random inheritance of epigenetic states plays a crucial role in stem cell differentiation and develop a hybrid model of stem cell differentiation induced by epigenetic modifications. Our model integrates a gene regulation network, epigenetic state inheritance, and cell regeneration to form multi-scale dynamics ranging from transcription regulation to cell population. Our simulation investigates how random inheritance of epigenetic states during cell division can automatically induce cell differentiation, dedifferentiation, and transdifferentiation. We show that interfering with epigenetic modifications or introducing extra transcription factors can regulate the probabilities of dedifferentiation and transdifferentiation, revealing the mechanism of cell reprogramming. This *in silico* model offers insights into the mechanism of stem cell differentiation and cell reprogramming.

Keywords: stem cell differentiation; epigenetic state; Waddington landscape; cell reprogramming; multi-scale model

1. Introduction

Adult stem cells are undifferentiated cells found throughout the body after development and multiply by cell division to replenish dying cells and regenerate damaged tissues[1]. The ability of well-controlled self-renewal and differentiation of adult stem cells is essential for tissue homeostasis. In stem cell biology,

*Corresponding author: jzlei@tiangong.edu.cn

it is significant to understand the regulation mechanism of self-renewal and differentiation of cells and to explore the determinants of cell fates.

Waddington's Landscape is a core concept in understanding the biological perspective of cell differentiation and cell fate decision[2]. A cell is considered as a small ball rolling in the mountain, and the downward scrolling of the ball represents the development pathway of the cell. Each valley represents a stable cell phenotype. As the ball rolls, the valley can be split into two new valleys by the ridge, representing the cell's fate choice with two possible new phenotypes. Waddington's landscape provides a visual metaphor for the development of multicellular organisms and is helpful for an intuitive understanding of the biological process; however, it remains argus on whether it matches the genuine situation of cell development[3]. Especially, how Waddington's landscape of a multicellular system is defined by the gene circuit that determined cell fates, what is the driving force of cell fate decision? How do the adult stem cell systems balance self-renewal and differentiation?

A gene circuit of two transcription factors (*e.g.*, PU.1-GATA1 or SOX2-OCT4) is a well-studied system that is associated with cell fate decisions[4, 5, 6]. This type of circuit consists of two genes, referring to two transcription factors, which can be self-activated and repressed by each other. Such gene network had been shown to have three stable equilibrium points through bifurcation analysis in the dynamical system, corresponding to three stable cell states (stem, differentiated fate 1, differentiated fate 2), which validates the view of Waddington's landscape. For example, in the PU.1-GATA1 gene circuit of hematopoietic stem cells, there is no significant difference in the expression of PU.1 and GATA1 in the precursor cells (stem cell state). However, high expression of PU.1 and the low expression of GATA1 promoted cells to become myeloid (differentiated cell fate 1), or conversely, high expression of GATA1 and low expression of PU.1 promoted the cells to become erythroid (differentiated cell fate 2). An analogous pattern is also seen in the SOX2-OCT4 circuit in embryonic stem cells, where SOX2 and OCT4 promote the neural ectoderm fate or mesoderm fate from the embryonic stem cell state, respectively. The above form of gene circuit motif is successively discovered in many living organisms[7, 8, 6, 9, 10, 11, 12], and hence provides a good example for exploring the mechanism of stem cell differentiation.

Given the landscape that defines the gene expression patterns of different types of cells, what is the driving force that triggers the process of cell type switches? Three possible mechanisms have been proposed to drive cell type switches[13]: stochastic fluctuation[14], gene regulation[15, 16, 17], and artificial induction (*e.g.*, induced pluripotent stem (iPS) cells)[18, 19, 20]. In living organisms, the differentiation of stem cells occurs automatically without external perturbations, and the resulting distribution of different types of cells can achieve a well-defined dynamic equilibrium in the face of random changes in environmental conditions. Therefore, regulating the cell type transition along with the natural process of stem cell regeneration is crucial for ensuring the reliable function of tissue cells.

In recent years, single-cell sequencing techniques have facilitated the study

of cell heterogeneity[21, 22, 23]. Gene expression can vary among cells with different phenotypes, indicating macro-heterogeneities[24]. Additionally, even cells considered the same phenotype can exhibit significant differences at the single-cell level, referred to as microscopic heterogeneity, which cannot be explained by known driving forces[24, 25, 26, 27]. Epigenetic regulation has been shown to play a crucial role in cellular heterogeneity and phenotype switching[28, 29, 30, 31].

Epigenetic regulation refers to non-genetic changes that can regulate gene expression, including DNA methylation, histone modifications, *etc.*. Histones are structural chromosome proteins, including H1 and polymers of H3, H4, H2A, and H2B. There were many forms and multiple functions of histone modifications to regulate gene expression. Trimethylation of lysine 4 on histone H3 protein subunit (H3K4me3) and H4K12 acetylation can promote gene expression, and ubiquitination such as ub-H2A can inhibit gene expression [32, 33]. Histone modifications were heritable during cell division. The parental modifications were recognized by a staining binding protein or a reading protein, while the reading protein recruited a chromatin modifier, or a writer protein to alter the histone modifications[34]. DNA methylation is an epigenetic mechanism that occurs by adding a methyl(CH_3) group to DNA, thereby often modifying the function of the genes and affecting gene expression. The inheritance of histone modifications and DNA methylation are somewhat semi-conservative but inevitably accompanied by natural changes during each generation, which may yield cell heterogeneity and plasticity[35].

Here, we established a hybrid model of stem cell regeneration with cell phenotype changes induced by epigenetic modifications. The model integrates a gene regulation network, epigenetic state inheritance, and cell regeneration to form multi-scale dynamics from transcription regulation to cell population. Through model simulations, we investigate how random inheritance of epigenetic state during cell division can automatically induce cell differentiation, dedifferentiation, and transdifferentiation. This study provides an *in silico* model that can help us to understand the mechanism of stem cell differentiation and cell reprogramming.

2. Hybrid model of stem cell differentiation

The hybrid model established in this study is illustrated in Figure 1. The model includes individual-based modeling of a multi-cellular system (Fig. 1A), in which the state of each cell is described with a gene regulation network (GRN) dynamics of two genes that are self-activated and repressed by each other (Fig. 1B), the dynamics of cell regeneration modeled with a G0 cell cycle model (Fig. 1C), and the stochastic inheritance of epigenetic state during cell division (Fig. 1D), Detailed formulations of the model are given below.

2.1. Gene regulation network

To investigate how epigenetic modification can drive cell lineage commitment, we consider a GRN that consists of two master transcription factors

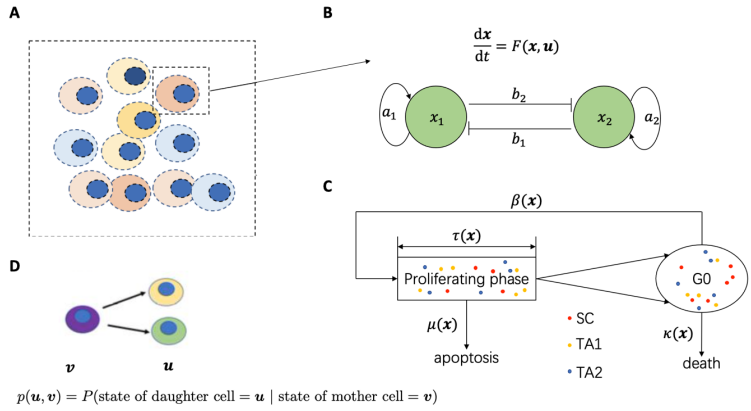

Figure 1: Illustration of the hybrid model. (A) Individual-based model of a multi-cellular system. (B) Dynamic system of gene circuit motif. (C) G0 cell cycle model of cell regeneration. (D) Stochastic inheritance of epigenetic state during cell division.

(TFs) X_1 and X_2, the two transcription factors are self-activated and repressed by each other (Fig. 1B). This gene network frequently arises in many systems of cell-fate decision-making and has been extensively studied[7, 8, 6, 9, 10, 11, 12].

Let x_1 and x_2 represent the expression level (protein concentration) of genes X_1 and X_2, respectively; the gene expression dynamics within one cell cycle are modeled with the following ordinary differential equations

$$\begin{cases} \dfrac{\mathrm{d}x_1}{\mathrm{d}t} = a_1 \left(\rho_1 + (1-\rho_1) \dfrac{x_1^n}{s_1^n + x_1^n} \right) + b_1 \dfrac{s_2^n}{s_2^n + x_2^n} - k_1 x_1, \\ \dfrac{\mathrm{d}x_2}{\mathrm{d}t} = a_2 \left(\rho_2 + (1-\rho_2) \dfrac{x_2^n}{s_2^n + x_2^n} \right) + b_2 \dfrac{s_1^n}{s_1^n + x_1^n} - k_2 x_2, \end{cases} \tag{1}$$

where a_1, a_2, ρ_1, ρ_2, s_1, s_2, n, b_1, b_2, k_1, k_2 are non-negative parameters. The parameters a_1 and a_2 denote the maximum expression rate of the self-activation of the two genes, ρ_1 and ρ_2 ($0 \leq \rho_i \leq 1$) represent the ratios between the basal level to the maximum level of the regulation of each gene. The parameters b_1 and b_2 denote the basal expression rate of the two genes without repression. The parameters s_1 and s_2 represent the half-effective concentration of the two proteins X_1 and X_2, respectively, in the transcription regulation. Degradation rates of the two proteins are represented by k_1 and k_2, respectively.

To incorporate the effects of epigenetic modification into the gene regulation dynamics, we note that epigenetic regulations (histone modification or DNA methylation) often interfere with chromatin structure and alter the basal expression levels. Hence, we assumed that the expression levels a_1 and a_2 depend on the epigenetic modification state of the two genes, presented by u_1 and u_2, respectively. Assuming that the epigenetic states mainly affect the chromatin structure and hence may alter the chemical potential to initiate the transcription

process, we can write the expression level a_1 and a_2 as

$$a_1(u_1) = \alpha_1 e^{\lambda_1 u_1}, \quad a_2(u_2) = \alpha_2 e^{\lambda_2 u_2}, \tag{2}$$

where α_1 and α_2 are positive parameters, and the coefficients $\lambda_i (i = 1, 2)$ represent the dependence of expression level to the epigenetic modification states. Here, $\lambda_i > 0$ means the epigenetic modification that increases the strength of self-activation, while $\lambda_i < 0$ means the epigenetic modification that reduces the strength of self-activation. Here, we assumed the epigenetic state $\boldsymbol{u} = (u_1, u_2) \in \Omega = [0, 1] \times [0, 1]$. Moreover, we assumed that the epigenetic states u_1 and u_2 only change randomly due to cell division, and is discussed below.

To consider the effects of extrinsic noise perturbation, we introduced stochastic fluctuations to a_1 and a_2, which are described as

$$a_1(u_1, \eta_1) = \alpha_1 e^{\lambda_1 u_1} e^{\sigma_1 \eta_1 - \sigma_1^2/2}, \quad a_2(u_2, \eta_2) = \alpha_2 e^{\lambda_2 u_2} e^{\sigma_2 \eta_2 - \sigma_2^2/2}, \tag{3}$$

where σ_1 and σ_2 represent the intensity of the noise perturbations, η_1 and η_2 are color noises defined by the Ornstein-Uhlenbeck processes

$$\mathrm{d}\eta_i = -(\eta_i/\zeta_i)\mathrm{d}t + \sqrt{2/\zeta_i}\mathrm{d}W_i(t), \quad (i = 1, 2), \tag{4}$$

where $W_1(t)$ and $W_2(t)$ are independent Wiener process, and ζ_1 and ζ_2 are relaxation coefficients. It is straightforward to have

$$\langle \eta_i(t_1)\eta_i(t_2)\rangle = e^{-|t_1 - t_2|/\zeta_i}$$

at the stationary state.

The above equations (1)-(4) give the random dynamics for the gene network in Figure 1B within one cell cycle. Given properly selected parameter values, the models can give rise to three stable steady states, each state represents a cell type (see Fig. 2 below). For example, the PU.1-GATA1 motif is included in the gene circuit that determines the cell fate of erythroid/megakaryocyte lineages from granulocyte/monocyte lineages. In this gene circuit, PU.1 and GATA1 are expressed in the precursor cells (PC). The granulocyte/monocyte lineage (GMC) cells show high PU.1 expression and low GATA1 expression, while erythroid/megakaryocyte lineage (EMC) cells show high GATA1 expression and PU.1 expression. In this study, for generality, the three cell types are named stem cell (SC), transit-amplifying cell 1 (TA1), and transit-amplifying cell 2 (TA2).

2.2. G0 cell cycle model

To incorporate the above gene regulation network dynamics with cell division, we referred to the G0 cell cycle model of heterogeneous cell regeneration [36, 37, 38]. In this model, we only consider cells with the ability of cell cycling, each cell has different rates of proliferation and cell death dependent on its epigenetic state. The cells that lost the ability to cell cycling are not considered and removed from the simulating pool. The cycling cells are classified into

resting (G0) or proliferating phases; resting phase cells can either re-enter the proliferating phase with a rate β or be removed from the resting phase with a rate κ due to cell death or senescence; proliferating phase cells can either lost randomly with a rate μ due to apoptosis or divide into two daughter cells at a time τ after entry into the proliferative compartment (Fig. 1C).

The state of each cell is represented by the expression level of marker genes X_1 and X_2, *i.e.*, $\boldsymbol{x} = (x_1, x_2)$, and the epigenetic state $\boldsymbol{u} = (u_1, u_2)$. The expression state $\boldsymbol{x}$ depends on the epigenetic state $\boldsymbol{u}$ within one cell cycle through equations (1)-(4). The expression state $\boldsymbol{x}$ determines the phenotype of a cell (SC, TA1, or TA2). The kinetic rates of each cell, including the proliferation rate β, the remove rate κ, the apoptosis rate μ, and the proliferation duration τ depend on the corresponding phenotype of a cell.

The SC and TA cells are different in their regulation of cell proliferation. Biologically, a stem cell's self-renewal ability is associated with microenvironmental conditions and intracellular signaling pathways [39, 40]. Despite the complex signaling pathways, the phenomenological formulation of Hill function dependence can be derived from simple assumptions regarding the interactions between signaling molecules and receptors [41, 37], and is given by

$$\beta(\boldsymbol{x}) = \beta_0 \frac{\theta}{\theta + Q(t)},$$

where $Q(t)$ represents the number of SC at time t, β_0 represents the maximum proliferation rate, and θ is a constant for the half-effective cell number. For TA cells that are fast amplifying, we simply assumed the maximum proliferation rate so that

$$\beta(\boldsymbol{x}) = \beta_0.$$

For SCs, define the removal rate κ, the apoptosis rate μ, and the proliferation duration τ of stem cells as

$$\kappa(\boldsymbol{x}) = \kappa_0, \quad \mu(\boldsymbol{x}) = \mu_0, \quad \tau(\boldsymbol{x}) = \tau_0.$$

For TA cells, we assumed that they have a higher removal rate and a shortened proliferation duration than stem cells. Moreover, each TA cell has a limited ability of cell divisions, *i.e.*, a TA cell will leave the simulating pool when it reaches the maximum cell division times (here we set it as 15). Hence, we have

$$\kappa(\boldsymbol{x}) = \begin{cases} 2\kappa_0, & \text{divisions} < 15, \\ +\infty, & \text{divisions} \geq 15, \end{cases} \qquad \mu(\boldsymbol{x}) = \mu_0, \quad \tau(\boldsymbol{x}) = \tau_0/2.$$

Table 1 summarizes the phenotypes of cells and the kinetic rates of cell cycling. See discussions of Figure 2 below for the phenotypes of cells.

From the above model description, given the epigenetic state $\boldsymbol{u} = (u_1, u_2)$ of each cell, the gene expression state $\boldsymbol{x} = (x_1, x_2)$ dynamically evolves according to the stochastic differential equations (1)-(4). Accordingly, the cell type and the kinetic rates $\beta(\boldsymbol{x})$, $\kappa(\boldsymbol{x})$, $\tau(\boldsymbol{x})$ and $\mu(\boldsymbol{x})$ can change during a cell cycle. In stochastic simulations, we model each cell's random proliferation, apoptosis,

Table 1: Phenotype of cells and the kinetic rates of cell cycling

cell type	(X_1, X_2)	$\beta(\boldsymbol{x})$	$\kappa(\boldsymbol{x})$	$\mu(\boldsymbol{x})$	$\tau(\boldsymbol{x})$
SC	$(+,+)$	$\beta_0\theta/(\theta+Q)$	κ_0	μ_0	τ_0
TA1	$(++,-)$	β_0	$2\kappa_0{}^{(a)}$	μ_0	$\tau_0/2$
TA2	$(-,++)$	β_0	$2\kappa_0{}^{(a)}$	μ_0	$\tau_0/2$

$^{(a)}$ when the division number less than 15.

and cell type switches in a multiple-cell system. Each cell has its cell state and randomly undergoes proliferation, apoptosis, and death with a probability depending on the cell state. Finally, when a cell undergoes mitosis, the cell divides into two cells, and the epigenetic states of the two daughter cells are calculated based on the inheritance probability functions given below.

2.3. Stochastic inheritance of epigenetic states

Histone modification and DNA methylations in the daughter cells are reconstructed during cell division following those in the mother cells. The epigenetic states of the daughter cells usually differ from those of their mother cells, and there is a random transition of the epigenetic states during cell division. Moreover, the molecules (proteins and mRNAs) in the mother cells undergo random partition during mitosis so that they are reallocated to the two daughter cells. Therefore, the epigenetic state $\boldsymbol{u}$ and the expression level (protein concentration) $\boldsymbol{x}$ of the model (1)-(4) for each newborn cell are reset after mitosis. Here, for simplicity, we assumed symmetry division so that the gene expression state $\boldsymbol{x}$ of the two daughter cells are the same as those of mother cells; however, the epigenetic state $\boldsymbol{u}$ may undergo random transition during cell division.

To model the stochastic inheritance of epigenetic states during cell division, we introduced an inheritance function $p(\boldsymbol{u}, \boldsymbol{v})$ to represent the conditional probability that a daughter cell of state $\boldsymbol{u}$ comes from a mother cell of state $\boldsymbol{v}$ after cell division, *i.e.*,

$$p(\boldsymbol{u}, \boldsymbol{v}) = P(\text{state of daughter cell} = \boldsymbol{u} \mid \text{state of mother cell} = \boldsymbol{v}).$$

The inheritance function represents cell plasticity in each cell cycle, while the detailed biochemical processes of cell division are ignored. It is obvious to have

$$\int_{\Omega} p(\boldsymbol{u}, \boldsymbol{v}) \mathrm{d}\boldsymbol{u} = 1, \quad \forall \boldsymbol{v} \in \Omega.$$

Biologically, the exact formulation of the inheritance function $p(\boldsymbol{u}, \boldsymbol{v})$ is difficult to determine, which is dependent on the complex biochemical reactions during the cell division process. Nevertheless, while we consider $p(\boldsymbol{u}, \boldsymbol{v})$ as a conditional probability density, we focus on the epigenetic state before and after cell division and omit the intermediate complex process. In this way, a phenomenological function can be introduced through numerical simulation based on a computational model of histone modification inheritance[37, 42, 43].

Assuming that the states u_1 and u_2 vary independently during cell division, we have

$$p(\boldsymbol{u}, \boldsymbol{v}) = p_1(u_1, \boldsymbol{v}) p_2(u_2, \boldsymbol{v}), \tag{5}$$

where $p_i(u_i, \boldsymbol{v})$ means the transition function of u_i, given the state $\boldsymbol{v}$ of the mother cell. According to [42, 43], the normalized nucleosome modification level of daughter cells can be described by a random beta-distribution number dependent on the mother cell. Thus, we wrote the inheritance function $p_i(u_i, \boldsymbol{v})$ through the density function of beta-distribution as

$$p_i(u_i, \boldsymbol{v}) = \frac{u_i^{g_i(\boldsymbol{v})-1}(1-u_i)^{h_i(\boldsymbol{v})-1}}{B(g_i(\boldsymbol{v}), h_i(\boldsymbol{v}))}, \quad B(g,h) = \frac{\Gamma(g)\Gamma(h)}{\Gamma(g+h)}, \tag{6}$$

where $\Gamma(z)$ is the gamma function, $g_i(\boldsymbol{v})$ and $h_i(\boldsymbol{v})$ are shape parameters that depend on the epigenetic state of the mother cell. We assumed that the conditional expectation and conditional variance of u_i are (given the state $\boldsymbol{v}$)

$$\mathrm{E}(u_i|\boldsymbol{v}) = \phi_i(\boldsymbol{v}), \quad \mathrm{Var}(u_i|\boldsymbol{v}) = \frac{1}{1+\psi_i(\boldsymbol{v})}\phi_i(\boldsymbol{v})(1-\phi_i(\boldsymbol{v})),$$

the shape parameters can be expressed as

$$g_i(\boldsymbol{v}) = \psi_i(\boldsymbol{v})\phi_i(\boldsymbol{v}), \quad h_i(\boldsymbol{v}) = \psi_i(\boldsymbol{v})(1-\phi_i(\boldsymbol{v})).$$

Here, we note that $\phi_i(\boldsymbol{v})$ and $\psi_i(\boldsymbol{v})$ always satisfy

$$0 < \phi_i(\boldsymbol{v}) < 1, \quad \psi_i(\boldsymbol{v}) > 0.$$

Hence, the inheritance function $p(\boldsymbol{u}, \boldsymbol{v})$ can be determined by the predefined conditional expectation and conditional variance, *i.e.*, the functions $\phi_i(\boldsymbol{u})$ and $\psi_i(\boldsymbol{u})$. Here, we assumed $\psi_i(\boldsymbol{v})$ a constant, and $\phi_i(\boldsymbol{v})$ an increase function of v_i and is expressed by a Hill function, *i.e.*,

$$\psi_i(\boldsymbol{v}) = m_0, \quad \phi_i(\boldsymbol{v}) = m_1 + m_2\frac{(m_3 v_i)^{m_4}}{1+(m_3 v_i)^{m_4}}, \quad \boldsymbol{v} = (v_1, v_2),\ i = 1, 2, \tag{7}$$

where $m_j (j = 0, 1, 2, 3, 4)$ are positive parameters.

From the above formulation, given the functions $\psi_i(\boldsymbol{v})$ and $\phi_i(\boldsymbol{v})$, the inheritance function $p(\boldsymbol{u}, \boldsymbol{v})$ can be given by the density function of beta- distribution random numbers.

2.4. Numerical scheme

The proposed hybrid model describes the dynamics of gene regulation networks and cell type switches of individual cells in a multicellular system. Here, we give an individual-based numerical scheme that aims at simulating the dynamics of each cell in the system.

- **Initialize** the time $t = 0$, the cell number N, and the state of all cells $\Sigma = \{[C_i(\boldsymbol{x}_i, \boldsymbol{u}_i)]_{i=1}^N\}$. Determine the phenotype (SC, TA1, or TA2) and the proliferation state (resting phase or proliferating phase) of all cells, and calculate the number Q of stem cells. All cells are initialized as stem cells and are at the resting phase. Accordingly, set the division number of each cell as $\text{div}_i = 0$, and the corresponding age at the proliferating phase (starting from the entry of proliferating phase) as $a_i = 0$.

- **for** t from 0 to T with step Δt **do**

  for each cell in Σ **do**

  * Numerically solve equations (1)-(4) for a step Δt, update the expression state $\boldsymbol{x}$. If the cell is at the resting phase, update the phenotype of the cell following the state $\boldsymbol{x}$.
  * Calculate the proliferation rate β, the apoptosis rate μ, the terminate differentiation rate κ, and the proliferation duration τ.
  * Determine the cell fate during the time interval $(t, t + \Delta t)$:
    · When the cell is at the resting phase, remove the cell from the simulating pool with a probability $\kappa\Delta t$, or enter the proliferating phase with a probability $\beta\Delta t$. If the cell enters the proliferating phase, set the age $a_i = 0$, and, if the cell is a TA cell, set $\text{div}_i = \text{div}_i + 1$.
    · When the cell is at the proliferating phase, if the age $a_i < \tau$, the cell is either removed (through apoptosis) with a probability $\mu\Delta t$, or remains unchanged and $a_i = a_i + \Delta t$; if the age $a_i \geq \tau$, the cell undergoes mitosis and divides into two cells. When mitosis occurs, set the state of two daughter cells following the rules below: set the age $a_i = 0$; set the epigenetic state $\boldsymbol{u}$ of each daughter cell according to the inheritance probability function $p(\boldsymbol{u}, \boldsymbol{v})$; set the gene expression state $\boldsymbol{x}$ as that of the mother cell.
    · After mitosis, check the division number of TA cells. If the division number div_i of a TA cell is larger than the maximum value, remove the cell from the simulating pool.

  end for

  Update the system Σ with the cell number, epigenetic and gene expression states of all surviving cells, and the ages of the proliferating phase cells, and set $t = t + \Delta t$.

  end for

The numerical scheme can be implemented by the object-oriented programming language `C++`.

Table 2 lists the parameter values used in the current study. Here, the parameters illustrate the general process of phenotype switches due to epigenetic

modifications along the cell regeneration process and do not refer to a specific type of cells. Moreover, we only limit our discussion to the situation of symmetric cells so that $b_1 = b_2, k_1 = k_2, s_1 = s_2, \rho_1 = \rho_2, a_1 = a_2$.

Table 2: Parameter values for model simulation

Parameter	Description	Value	Unit[(a)]
b_1, b_2	Strengths of the mutual inhibition	1	AU $\times$ h^{-1}
k_1, k_2	Degradation rates of the proteins	1	AU $\times$ h^{-1}
s_1, s_2	50% effective concentration of the feedback loops	0.5	AU
ρ_1, ρ_2	The ratio between the basal level to the maximum level of the regulation of each gene	0.1	-
σ_1, σ_2	Intensity of the noise	0.05	-
ζ_1, ζ_2	Relaxation coefficient of the Ornstein-Uhlenbeck process	1	h^{-1}
α_1, α_2	constant	0.4	AU $\times$ h^{-1}
λ_1, λ_2	Expression rate of each gene	1.9	-
n	Hill coefficient	4	-
m_0	constant	60	-
m_1	constant	0.08	-
m_2	constant	1.0	-
m_3	constant	1.65	-
m_4	Hill coefficient	1.8	-
θ	Constant for the half-effective cell number for SC population control	200	cells
β_0	Maximum proliferation rate	0.04	h^{-1}
κ_0	The rate of removing cells out of the resting phase	0.01	h^{-1}
μ_0	The apoptosis rate of cells in the proliferating phase	0.0002	h^{-1}
τ_0	Proliferating phase time	5	h

[(a)] AU means arbitrary unit.

3. Results

3.1. Phenotype defined by the epigenetic state of cells

To quantitatively define the phenotypes of SC and TA cells based on the gene expression state $\boldsymbol{x} = (x_1, x_2)$, we perform bifurcation analysis for the ordinary differential equation (1). Here, we assumed the symmetric situation so that $a_1 = a_2 = a$ and considered the bifurcation concerning the expression rate a. Figure 2A shows the dependence of the equilibrium state on the parameter a. When a is large ($a > 1.65$), there is a stable state steady with high expressions in both

X_1 and X_2, which is denoted as $(+,+)$. When a decreases ($0.75 < a < 1.65$), in addition to the state $(+,+)$, there are two other stable steady states, one state has high expression in X_1 and low expression in X_2; the other one is opposite with low expression in X_1 and high expression in X_2. We denote these two states as $(++,-)$ and $(-,++)$, respectively. When a further decreases ($a < 0.75$), the state $(+,+)$ vanishes, and the two states $(++,-)$ and $(-,++)$ persist. Biologically, when a decreases from a large ($a > 1.65$) to a small ($a < 0.75$) value, the cell type $(+,+)$ emerge firstly, followed by the coexistence of the three states, and finally, transit to the cell type of either $(++,-)$ or $(-,++)$. This is akin to the differentiation of precursor cells to either granulocyte/monocyte lineage or erythroid/megakaryocyte lineage described with the PU.1-GATA1 gene circuit of hematopoietic stem cells. Thus, we consider the state $(+,+)$ as stem cells (SC), while the states $(++,-)$ and $(-,++)$ are downstream transit-amplifying cells (TA1 and TA2). This gives the phenotypes of cells in Table 1. Moreover, Figure 2A implies the following definition of cell types from $\boldsymbol{x} = (x_1, x_2)$ as:

$$\text{phenotype} = \begin{cases} \text{SC}: & \text{if } x_1 > 0.5, x_2 > 0.5, \\ \text{TA1}: & \text{if } x_1 > 0.5, x_2 < 0.5, \\ \text{TA2}: & \text{if } x_1 < 0.5, x_2 > 0.5. \end{cases}$$

Considering the effects of epigenetic modifications and extrinsic noise perturbations, the expression rates a_i are expressed as (3). First, we take $\alpha_1 = \alpha_2 = 0.4, \lambda_1 = \lambda_2 = 1.9$ and omit the extrinsic noise by setting $\sigma_1 = \sigma_2 = 0$, the dependence of the phenotypes of steady state on the epigenetic state u_1 and u_2 is shown in Figure 2B. Figure 2B suggests that the three cell types SC, TA1, or TA2 may occur when the epigenetic states of the two genes vary. Specifically, the stem cell state can emerge when $u_1 > 0.4$ and $u_2 > 0.4$.

Next, we set $\sigma = 0.05$ to introduce the noise perturbation. In this case, the gene expression dynamics is described by the random differential equations (1)-(4). To explore the dynamics of cell-type transition under noise perturbations, given the epigenetic state u_1 and u_2, we set the initial condition following Figure 2B and numerically solve equations (1)-(4) for 100 h. Simulations show that TA cells remain unchanged during the simulation. However, for SC with (u_1, u_2) take values near the edge of the SC zone, the cell can switch to TA cell following random perturbations (Fig. 2C). Figure 2D shows the average duration of the SC state with different epigenetic states (u_1, u_2). These results indicate that the definition of cell types of SC, TA1, and TA2 is proper following the gene regulation dynamics (1)-(4), and the epigenetic state (u_1, u_2) is important for the phenotype of cells.

3.2. Population dynamics of stem cell regeneration and differentiation

To investigate the population dynamics of stem cell regeneration and differentiation, we considered the full model introduced in Section 2. First, we run the model simulation with initially 100 cells, the epigenetic state $\boldsymbol{u}$ and gene expression state $\boldsymbol{x}$ of each cell are random over the range $0 < u_i < 1$

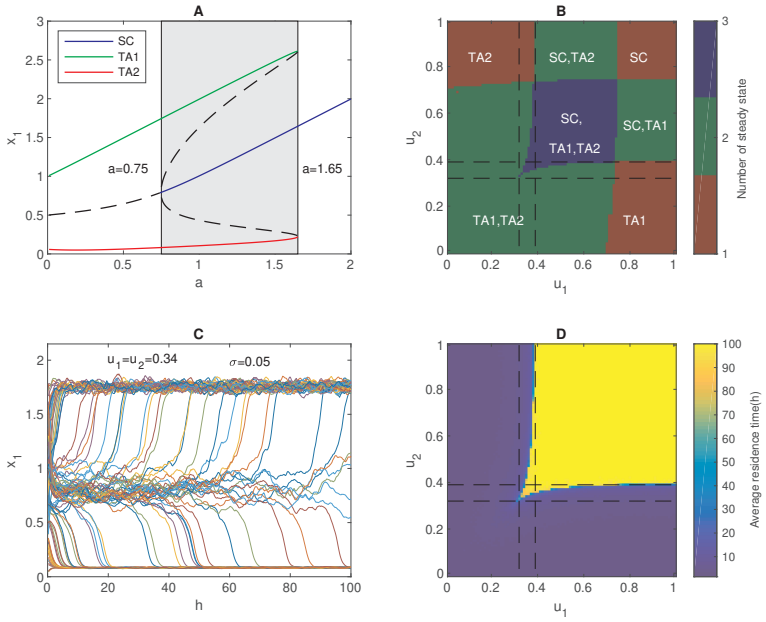

Figure 2: Bifurcation analysis of the gene expression dynamics. (A) Dependence of the steady state solution (in x_1) on the expression rate a ($a_1 = a_2 = a$). Solid lines represent stable steady states; the blue line is for SC, the green line is for TA1, and the red line is for TA2. Dashed lines represent unstable steady states. (B) Dependence of the cell types with epigenetic states u_1 and u_2. Here $\alpha_1 = \alpha_2 = 0.4$ and $\lambda_1 = \lambda_2 = 1.9$. The color shows the number of steady states. (C) Sample dynamics of cell state transition obtained by solving the stochastic differentiation equation (1)-(4). Here $u_1 = u_2 = 0.34$, $\sigma = 0.05$. (D) Average duration of the SC state with the epigenetic state (u_1, u_2).

and $0 < x_i < 3$, respectively. To examine the population dynamics with different expression rates of the two genes, we test 4 sets of parameters, with $(\alpha_1, \alpha_2) = (0.4, 0.4), (0.4, 1.0), (1.0, 0.4)$ and $(1.0, 1.0)$, respectively, and for each set of parameters, run the model to 2000 h. In each case, the cells undergo proliferation, differentiation, and cell death, so the populations of SC and TA cells approach homeostasis. Figure 3 shows the 4 types of population dynamics for different sets of parameters. When $(\alpha_1, \alpha_2) = (0.4, 0.4)$, the SC and both TA1 and TA2 cells coexist, which implies the process of self-renewal of stem cells and the differentiation of SC to TA1 and TA2 (Fig. 3A). When $(\alpha_1, \alpha_2) = (0.4, 1.0)$, only SC and TA2 cells exist, and there are no TA1 cells at homeostasis, which indicates the blockage of the differentiation from stem cells to TA1 cells (Fig. 3B). Similarly, when $(\alpha_1, \alpha_2) = (1.0, 0.4)$, there are no TA2 cells at homeostasis (Fig. 3C), which indicates the blockage of the differentiation from stem cells to TA2 cells. When $(\alpha_1, \alpha_2) = (1.0, 1.0)$, only stem cells exist at homeostasis, and no events of stem cell differentiation occur during the simulation (Fig. 3D). These results indicate that kinetic parameters of the underlying gene regulation dynamics are crucial for cell phenotypes in homeostasis. In this study, we are interested in coexistence with SC, TA1, and TA2 cells, and hence take $(\alpha_1, \alpha_2) = (0.4, 0.4)$ in the following discussions.

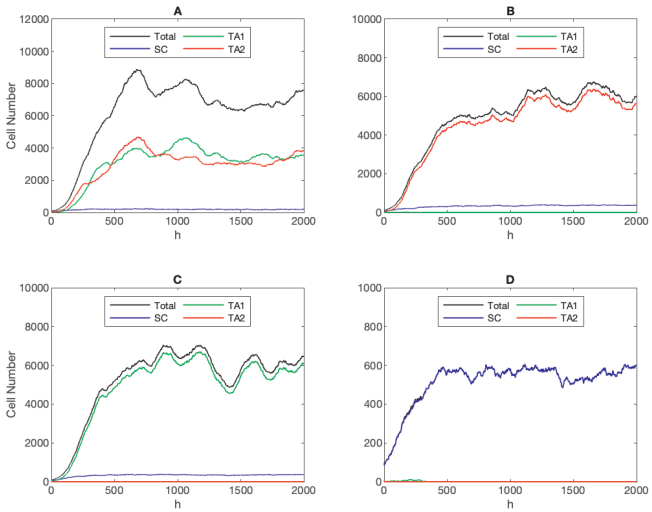

Figure 3: Population dynamics of stem cell regeneration and differentiation. Figures show the evolution dynamics of SC and TA cells number, with different sets of parameters: (A) $(\alpha_1, \alpha_2) = (0.4, 0.4)$, (B) $(\alpha_1, \alpha_2) = (0.4, 1.0)$, (C) $(\alpha_1, \alpha_2) = (1.0, 0.4)$, (D) $(\alpha_1, \alpha_2) = (1.0, 1.0)$. Other parameters remained the same as in Table 2.

Now, we further investigate the molecular level dynamics of individual cells. Figure 4A shows the scatter plots of $\boldsymbol{x} = (x_1, x_2)$ of all cells at different time points ($t = 1, 50, 1000, 1000$h). The initially randomly distributed cell states

rapidly develop into three clusters of SC, TA1, and TA2 cells. Accordingly, the epigenetic state $\boldsymbol{u} = (u_1, u_2)$ of cells rapidly converges to the steady distribution at homeostasis (Fig. 4B). Interestingly, despite the continuous distribution of (u_1, u_2), the expression states (x_1, x_2) show discrete cell types at homeostasis. From the bifurcation analysis in Figure 2, continuous change in the epigenetic state $\boldsymbol{u}$ can lead to a transition of cell types that are defined by the gene expression state $\boldsymbol{x}$. These results indicate that continuous change in the epigenetic state during stem cell regeneration can lead to discontinuous cell fate decisions. This gives the mechanism of stem cell differentiation driven by random inheritance of epigenetic state during cell division.

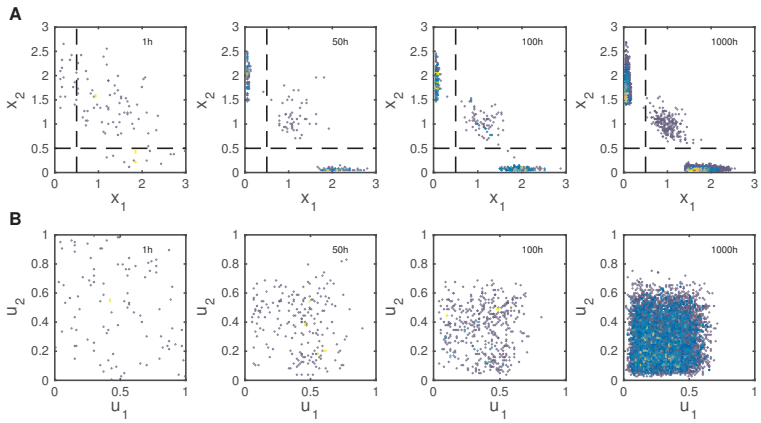

Figure 4: The evolution of gene and epigenetic modification for the population dynamics shown in Figure 3A. (A) The scatter plots of (x_1, x_2) at time = 1h, 50h, 100h, 1000h. (B)The scatter plots of (u_1, u_2) at time = 1h, 50h, 100h, 1000h.

3.3. Dynamics of transdifferentiation and dedifferentiation

The above simulations show differentiation dynamics from stem cells to TA cells, normally occurring during development and tissue homeostasis. Nevertheless, transdifferentiation and dedifferentiation are also seen in many biological processes, during which differentiated cells may lose the phenotype and convert to another cell type or the undifferentiated state [15, 44, 45, 46]. Here, we have seen that random inheritance of epigenetic states can induce the differentiation of stem cells. We further asked whether this mechanism can induce transdifferentiation and dedifferentiation. To this end, we recorded the cell type changes over a long simulation and counted the number of events of cell type changes in each cell division. The results are summarized as the transition probability in each cell division in Table 3.

From the results in Table 3, stem cells under self-renewal with a probability of 74.46% or transit to either TA1 or TA2 cells with a probability of 12.95% or 12.58%, respectively, during each cell cycle. The TA cells, however, are mostly self-renewal with a probability higher than 99.99%. Nevertheless,

the rare events of transdifferentiation (from TA1 to TA2 or from TA2 to TA1) and dedifferentiation (from TA1 or TA2 to SC) do happen in our simulations, despite the extremely low frequencies. Here, we note that the transition probabilities depend on the model parameters. In the next section, we discuss how changes in model parameters may affect the frequencies of transdifferentiation and dedifferentiation. Figure 5 shows the dynamics of transdifferentiation and dedifferentiation from our model simulation.

Table 3: Cell state transition probabilities from mother to daughter cells at one cell division.

	SC	TA1	TA2
SC	0.7446	0.1295	0.1258
TA1	7.87×10^{-6}	0.999967	2.52×10^{-5}
TA2	1.45×10^{-5}	8.85×10^{-6}	0.999977

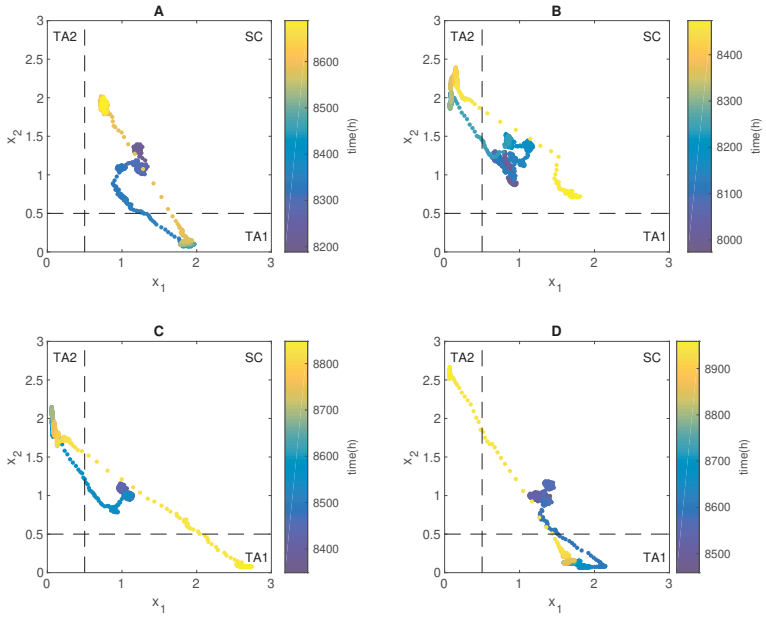

Figure 5: Transition dynamics of differentiation, dedifferentiation, and transdifferentiation. (A) The trajectory SC-TA1-SC. (B) The trajectory SC-TA2-SC. (C) The trajectory SC-TA2-TA1. (D) The trajectory SC-TA1-TA2. Color bars show the timing in the simulation.

3.4. The effects of extrinsic noise and epigenetic state inheritance on homeostasis and cell type transitions

Now, we discuss the effects of extrinsic noise and epigenetic state inheritance on the system homeostasis and the probabilities of cell type transitions.

First, we varied noise perturbation strength σ from 0 to 0.2 and examined the homeostasis cell numbers and the transition probabilities. For each value of σ,

we performed a model simulation for a time scope of 10000h and took the results from 4000h to 10000h for further analysis. Similar to the previous simulations, the cells develop into either SC or TA cells and approach homeostasis following model simulations. The numbers of different types of cells at homeostasis are insensitive to the change in the noise strength (Fig. 6A), and the ratios of different types of cells are unaffected by the noise strength neither (Fig. 6B). These results suggest that changes in the extrinsic noise do not affect the system state at homeostasis.

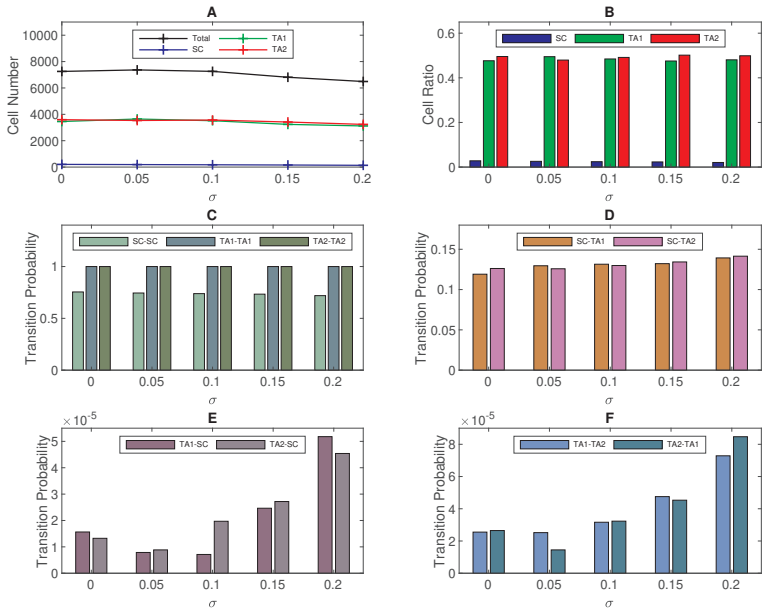

Figure 6: The effect of extrinsic noise on homeostasis and cell state transition. (A) Numbers of different types of cells at homeostasis. (B) Ratios of SC and TA cells at homeostasis. (C) The probability of self-renewal in each cell division of different types of cells. (D) The probability of differentiation (SC-TA1, SC-TA2) in each cell division. (E) The probability of dedifferentiation (TA1-SC, TA2-SC) in each cell division. (F) The probabilities of transdifferentiation (TA1-TA2, TA2-TA1) in each cell division. All values are calculated from the time scope of 4000h to 10000h in the model simulation.

We further investigate the transition probabilities between different cell types; the results are shown in Figure 6C-F. The probabilities of self-renewal (SC-SC, TA1-TA1, TA2-TA2) are unaffected by the changes in the noise strength (Fig. 6C). The probabilities of differentiation (SC-TA1 and SC-TA2) are mostly unchanged when the noise strength σ is small ($\sigma \leq 0.05$), and slightly increase when σ becomes larger ($\sigma \geq 0.1$) (Fig. 6D), which are compensated with the slight increases in the probabilities of dedifferentiation (TA1-SC and TA2-SC) (Fig. 6E) so that the ratios of cells remain unchanged. Similarly, the probabilities of transdifferentiation (TA1-TA2 and TA2-TA1) are insensitive to the extrinsic noise under weak noise ($\sigma \leq 0.1$), and a slight increase under strong perturbation ($\sigma \geq 0.15$). These results suggest that extrinsic noise perturbation

might not be the main driven force of cell-type transitions.

Next, we investigated how random changes in epigenetic modifications may affect the system homeostasis and cell type transitions. To this end, we considered the functions $\phi_i(\boldsymbol{v})$ in (7) that defines the inheritance function of epigenetic states. We varied the parameter m_2 over the interval $[0.8, 0.9]$ and investigated how the cell numbers and transition probabilities may change with m_2. Here, we fixed $\sigma = 0.05$ and other parameters remained the same as in Table 2. Simulations show that the numbers of TA cells decrease with the increase of m_2, and the SC number increases with m_2. As a result, the total cell number decreases with m_2 (Fig. 7A). Accordingly, the ratio of SC increases with m_2, along with the decrease of TA1 and TA2 ratios (Fig. 7B). These results suggest that alterations in the inheritance functions of epigenetic states can significantly impact the homeostasis of the system.

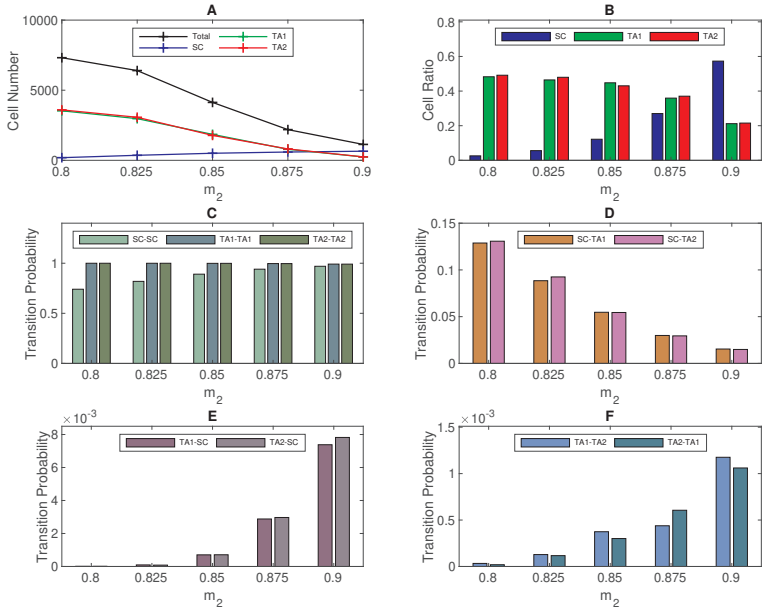

Figure 7: The effect of epigenetic state inheritance function on homeostasis and cell state transition. (A) Numbers of different types of cells at homeostasis. (B) Ratios of SC and TA cells at homeostasis. (C) The probability of self-renewal in each cell division of different types of cells. (D) The probability of differentiation (SC-TA1, SC-TA2) in each cell division. (E) The probability of dedifferentiation (TA1-SC, TA2-SC) in each cell division. (F) The probabilities of transdifferentiation (TA1-TA2, TA2-TA1) in each cell division. All values are calculated from the time scope of 4000h to 10000h in the model simulation.

We further investigate the probability of cell differentiation, transdifferentiation, and dedifferentiation. The probabilities of self-renewal for TA cells are mostly unaffected by changes in m_2; however, the self-renewal probability of SC increases m_2 (Fig. 7C). Accordingly, the differentiation probabilities (SC-TA1 and SC-TA2) obviously decrease with m_2 (Fig. 7D), and the dedifferentiation

probabilities (TA1-SC and TA2-SC) increase with m_2 (Fig. 7E). The transdifferentiation probabilities (TA1-TA2 and TA2-TA1) also increase with m_2. Biologically, the function $\phi_i(\boldsymbol{v})$ means the expectation of the epigenetic state of daughter cells given the state $\boldsymbol{v}$ of the mother cells. Increasing the parameter m_2 means upregulating the daughter cells' epigenetic states u_i. These results suggest a way of inducing transdifferentiation and dedifferentiation by interfering with epigenetic modifications.

3.5. Dynamics of cell reprogramming through the induction of transcription factors

The above simulations have discussed the mechanisms of cell transdifferentiation and dedifferentiation through the induction of extrinsic noise and interfering with epigenetic modification. Here, we further applied the model to study the dynamics of cell reprogramming through the induction of transcription factors.

We assumed an external transcription factor that increases the transcription of the self-activation of the X_1 gene. Thus, equations of the gene regulation network dynamics were rewritten as

$$\begin{cases} \dfrac{\mathrm{d}x_1}{\mathrm{d}t} = (a_1 + a_{TF})(\rho_1 + (1-\rho_1)\dfrac{x_1^n}{s_1^n + x_1^n}) + b_1 \dfrac{s_2^n}{s_2^n + x_2^n} - k_1 x_1, \\ \dfrac{\mathrm{d}x_2}{\mathrm{d}t} = a_2(\rho_2 + (1-\rho_2)\dfrac{x_2^n}{s_2^n + x_2^n}) + b_2 \dfrac{s_1^n}{s_1^n + x_1^n} - k_2 x_2. \end{cases} \tag{8}$$

Here, the extra factor a_{TF} denotes the increasing activation rate caused by the introduced transcription factor.

To simulate the dynamics of cell reprogramming, we fixed $\sigma = 0.05$, $m_2 = 0.8$ and varied a_{TF} from 0 to 0.4, and other parameters were the same as in Table 2. We initialized the cells with differentiated states (TA1 or TA2 cells) and performed model simulations to examine the population dynamics of different types of cells and the cell type transition probabilities. In the population dynamics shown in Figure 8A, in which the cells were initialized as TA2 cells, stem cells start to appear at about 300h following the dedifferentiation of TA2 cells. Next, stem cells differentiate into TA1 and TA2 cells, so the cell population approaches homeostasis with all three types of cells. We varied the factor a_{TF} and examine the ratios of different cell types at homeostasis, the ratios of TA1 cells and stem cells increase with a_{TF}, and the ratio of TA2 cells decreases with a_{TF} (Fig. 8B). We further compare the transition probability with different values of a_{TF}. The probability of self-renewal at each cell division is unaffected with a_{TF}; however, changes in a_{TF} obviously affect the probabilities of differentiation, transdifferentiation, and dedifferentiation. An increase in a_{TF} can reduce the differentiation from SC to TA1 cells, promote the dedifferentiation from TA2 cells to SC, and alter the transdifferentiation between TA1 and TA2 cells, with an increase in the TA2-TA1 transition and a decrease in the TA1-TA2 transition (Fig. 8C-F).

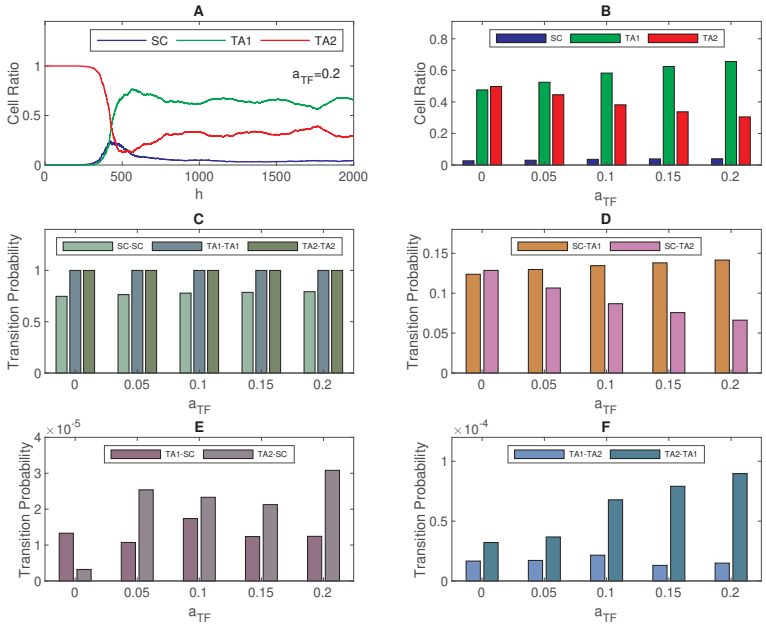

Figure 8: The effect of transcription factor introduction on cell number and cell state transition. (A) Time evolution of the cell ratios starting from a TA2 cell population. (B) The cell ratios for different types of cells over the time period from 4000h to 10000h. (C)-(F)The cell transition probabilities.

3.6. Waddington landscape

To further investigate how extrinsic noise and epigenetic state inheritance may affect cell fate decisions during tissue growth, we calculate the temporal evolution of Waddington landscape based on simulation results. The above numerical scheme gives the number $N(t, \boldsymbol{x})$ of cells at time t with state $\boldsymbol{x} = (x_1, x_2)$. The total cell number is given by $N(t) = \int N(t, \boldsymbol{x})\mathrm{d}\boldsymbol{x}$. Accordingly, $f(t, \boldsymbol{x}) = N(t, \boldsymbol{x})/N(t)$ gives the frequency of cells with state $\boldsymbol{x}$. Thus, the evolution of Waddington's epigenetic landscape can be defined as

$$U(t, \boldsymbol{x}) = -\log(1 + f(t, \boldsymbol{x})), \tag{9}$$

the number 1 is introduced to avoid the issue of zero frequency.

Figure 9 displays landscapes with varying extrinsic noise σ, epigenetic regulation parameter m_2, and extra factor a_{TF} in cell reprogramming. As shown in Figure 9A, the landscape is insensitive to changes in the extrinsic noise strength, which is consistent with the above discussion that changes in the extrinsic noise do not affect the system state of homeostasis (Fig. 6). However, the landscapes exhibit significant changes when the parameter m_2 increases from 0.8 to 0.9 (Fig. 9B). Increasing m_2 results in a higher ratio of stem cells at the stationary state, implying the induction of dedifferentiation through changes in epigenetic regulation. Introduction of the extra factor a_{TF} in (8) can disrupt the balance between TA1 and TA2 cells, leading to a higher fraction of TA1 cells (Fig. 9C). These results highlight the significant roles of varying epigenetic regulation and introducing an extra transcription factor in altering the Waddington landscape.

4. Discussion

The regulation of stem cell differentiation and tissue development is a fundamental problem in developmental biology and regenerative medicine. Various mechanisms have been proposed to induce biological processes such as cell differentiation, dedifferentiation, and transdifferentiation. These driven forces include stochastic fluctuation, alteration of gene regulation networks, induction of external transcription factors, or induction by small molecules. However, these driven forces are exogenous and cannot explain the natural evolution of cell lineage or cellular heterogeneity. In recent years, the impact of epigenetic regulation on cellular heterogeneity and phenotype switches has been widely recognized.

To quantitatively study the dynamics of cell type transition mediated by epigenetic modifications, we developed a hybrid model of stem cell regeneration that integrates gene regulation networks, epigenetic state inheritance, and cell regenerations. Our model simulates the biological process of cell population growth and homeostasis formation with a balance between different types of cells. Our simulations demonstrate a mechanism whereby stochastic epigenetic modification inheritance induces spontaneous phenotype switches during cell cycling, and the crosstalk between random epigenetic transition and intrinsic

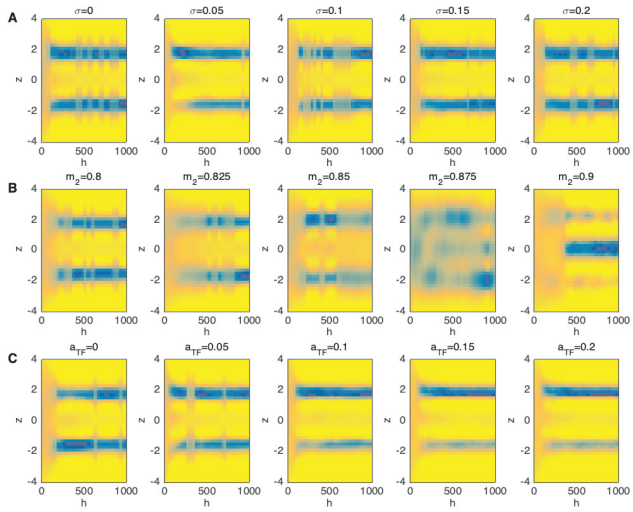

Figure 9: Waddington landscape. (A) Temporal evolution of Waddington landscape with varying extrinsic noises. (B) Temporal evolution of Waddington landscape with varying epigenetic regulation parameter m_2. (C) Temporal evolution of Waddington landscape with varying extra factor a_{TF} in cell reprogramming. Here, the Waddington landscapes are shown by heatmaps for the function $U(t, z)$ with $z = x_1 - x_2$.

gene network dynamics plays essential roles in cell type switches and stabilization. Moreover, our results show that modifications in epigenetic regulation can alter the epigenetic landscape and increase the potential of cell dedifferentiation and/or transdifferentiation.

The Waddington landscape is a fundamental concept in stem cell differentiation and cell plasticity. Typically, the stochastic dynamics of a gene regulatory network are formulated as Langevin equations or the associated master equation or Fokker-Planck equation. The Waddington landscape at homeostasis can be expressed as the potential $U = -\ln(P_{ss})$ using the stationary distribution P_{ss} of the master equation or Fokker-Planck equation. Minimizing the potential U provides the phenotypes associated with the underlying regulatory network. However, the potential U does not incorporate the dynamics of cell type switches associated with development and tissue growth. In our study, we propose a computational model that combines cell regeneration and epigenetic modifications during cell division to quantify the relationship between alterations in the epigenetic landscape and corresponding phenotypic changes. Through model simulation, the temporal potential of a biological system can be defined, which provides a technique to investigate the evolutionary dynamics of the Waddington landscape during tissue growth. Our work provides novel insights into the mechanisms of stem cell differentiation and cell reprogramming and may have important implications for regenerative medicine.

Acknowledgements

This work is supported by the National Natural Science Foundation of China 11831015.

References

[1] H. Clevers, What is an adult stem cell?, Science (New York, NY) 350 (6) (2015-12) 1319 – 1320. doi:10.1126/science.aad7016.

[2] C. H. Waddington, The epigenotype, International journal of epidemiology 41 (1) (2012) 10–13. doi:10.1093/ije/dyr184.

[3] J. E. Ferrell, Bistability, bifurcations, and Waddington's epigenetic landscape, Current Biology 22 (11) (2012) R458–R466. doi:10.1016/j.cub.2012.03.045.
URL `http://dx.doi.org/10.1016/j.cub.2012.03.045`

[4] J. Wang, K. Zhang, L. Xu, E. Wang, Quantifying the Waddington landscape and biological paths for development and differentiation, Proceedings of the National Academy of Sciences 108 (20) (2011) 8257–8262. doi:10.1073/pnas.1017017108.
URL `http://www.pnas.org/cgi/doi/10.1073/pnas.1017017108`

[5] N. Iovino, G. Cavalli, Rolling ES cells down the waddington landscape with Oct4 and Sox2, Cell 145 (6) (2011) 815–817. doi:10.1016/j.cell.2011.05.027.
URL `http://dx.doi.org/10.1016/j.cell.2011.05.027`

[6] J. X. Zhou, S. Huang, Understanding gene circuits at cell-fate branch points for rational cell reprogramming, Trends in Genetics 27 (2) (2011) 55–62. doi:10.1016/j.tig.2010.11.002.
URL `http://dx.doi.org/10.1016/j.tig.2010.11.002`

[7] H. Niwa, Y. Toyooka, D. Shimosato, D. Strumpf, K. Takahashi, R. Yagi, J. Rossant, Interaction between Oct3/4 and Cdx2 determines trophectoderm differentiation, Cell 123 (5) (2005) 917–929. doi:10.1016/j.cell.2005.08.040.

[8] A. E. Schaffer, K. K. Freude, S. B. Nelson, M. Sander, Nkx6 transcription factors and Ptf1a function as antagonistic lineage determinants in multipotent pancreatic progenitors, Developmental Cell 18 (6) (2010) 1022–1029. doi:10.1016/j.devcel.2010.05.015.
URL `http://dx.doi.org/10.1016/j.devcel.2010.05.015`

[9] A. Ralston, J. Rossant, Genetic regulation of stem cell origins in the mouse embryo, Clinical Genetics 68 (2) (2005) 106–112. doi:10.1111/j.1399-0004.2005.00478.x.

[10] S. H. Orkin, L. I. Zon, Hematopoiesis: An Evolving Paradigm for Stem Cell Biology, Cell 132 (4) (2008) 631–644. doi:10.1016/j.cell.2008.01.025.

[11] Y. H. Loh, J. H. Ng, H. H. Ng, Molecular framework underlying pluripotency, Cell Cycle 7 (7) (2008) 885–891. doi:10.4161/cc.7.7.5636.

[12] J. Wang, L. Xu, E. Wang, S. Huang, The potential landscape of genetic circuits imposes the arrow of time in stem cell differentiation, Biophysical Journal 99 (1) (2010) 29–39. doi:10.1016/j.bpj.2010.03.058.

[13] L. Xu, K. Zhang, J. Wang, Exploring the mechanisms of differentiation, dedifferentiation, reprogramming and transdifferentiation, PLoS ONE 9 (8). doi:10.1371/journal.pone.0105216.

[14] R. Losick, C. Desplan, Stochasticity and cell fate, Science 320 (5872) (2008) 65–68. doi:10.1126/science.1147888.

[15] C. Cobaleda, W. Jochum, M. Busslinger, Conversion of mature B cells into T cells by dedifferentiation to uncommitted progenitors, Nature 449 (7161) (2007) 473–477. doi:10.1038/nature06159.

[16] Q. Zhou, D. A. Melton, Extreme Makeover: Converting One Cell into Another, Cell Stem Cell 3 (4) (2008) 382–388. doi:10.1016/j.stem.2008.09.015.

[17] Q. Zhou, J. Brown, A. Kanarek, J. Rajagopal, D. A. Melton, In vivo reprogramming of adult pancreatic exocrine cells to β-cells, Nature 455 (7213) (2008) 627–632. doi:10.1038/nature07314.

[18] S. Yamanaka, Induced pluripotent stem cells: Past, present, and future, Cell Stem Cell 10 (6) (2012) 678–684. doi:10.1016/j.stem.2012.05.005.
URL `http://dx.doi.org/10.1016/j.stem.2012.05.005`

[19] G. Amabile, A. Meissner, Induced pluripotent stem cells: current progress and potential for regenerative medicine, Trends in Molecular Medicine 15 (2) (2009) 59–68. doi:10.1016/j.molmed.2008.12.003.

[20] J. Shu, C. Wu, Y. Wu, Z. Li, S. Shao, W. Zhao, X. Tang, H. Yang, L. Shen, X. Zuo, W. Yang, Y. Shi, X. Chi, H. Zhang, G. Gao, Y. Shu, K. Yuan, W. He, C. Tang, Y. Zhao, H. Deng, Induction of Pluripotency in Mouse Somatic Cells with Lineage Specifiers, Cell 153 (5) (2013) 963–975. doi:10.1016/j.cell.2013.05.001.
URL `http://dx.doi.org/10.1016/j.cell.2013.05.001`
`https://linkinghub.elsevier.com/retrieve/pii/S009286741300531X`

[21] C. Angermueller, S. J. Clark, H. J. Lee, I. C. Macaulay, M. J. Teng, T. X. Hu, F. Krueger, S. A. Smallwood, C. P. Ponting, T. Voet, G. Kelsey, O. Stegle, W. Reik, Parallel single-cell sequencing links transcriptional and epigenetic heterogeneity, Nature Methods 13 (3) (2016) 229–232. doi:10.1038/nmeth.3728.

[22] A. A. Pollen, T. J. Nowakowski, J. Shuga, X. Wang, A. A. Leyrat, J. H. Lui, N. Li, L. Szpankowski, B. Fowler, P. Chen, N. Ramalingam, G. Sun, M. Thu, M. Norris, R. Lebofsky, D. Toppani, D. W. Kemp, M. Wong, B. Clerkson, B. N. Jones, S. Wu, L. Knutsson, B. Alvarado, J. Wang, L. S. Weaver, A. P. May, R. C. Jones, M. A. Unger, A. R. Kriegstein, J. A. West, Low-coverage single-cell mRNA sequencing reveals cellular heterogeneity and activated signaling pathways in developing cerebral cortex, Nature Biotechnology 32 (10) (2014) 1053–1058. doi:10.1038/nbt.2967.

[23] A. P. Patel, I. Tirosh, J. J. Trombetta, A. K. Shalek, S. M. Gillespie, H. Wakimoto, D. P. Cahill, B. V. Nahed, W. T. Curry, R. L. Martuza, D. N. Louis, O. Rozenblatt-Rosen, M. L. Suvà, A. Regev, B. E. Bernstein, Single-cell RNA-seq highlights intratumoral heterogeneity in primary glioblastoma, Science 344 (6190) (2014) 1396–1401. doi:10.1126/science.1254257.

[24] S. Huang, Non-genetic heterogeneity of cells in development: More than just noise, Development 136 (23) (2009) 3853–3862. doi:10.1242/dev.035139.

[25] A. K. Björklund, M. Forkel, S. Picelli, V. Konya, J. Theorell, D. Friberg, R. Sandberg, J. Mjösberg, Erratum: The heterogeneity of human CD127+ innate lymphoid cells revealed by single-cell RNA sequencing (Nature Immunology (2016) 17 (451-460)), Nature Immunology 17 (6) (2016) 740. doi:10.1038/ni0616-740a.
URL `http://dx.doi.org/10.1038/ni0616-740a`

[26] M. B. Johnson, P. P. Wang, K. D. Atabay, E. A. Murphy, R. N. Doan, J. L. Hecht, C. A. Walsh, Single-cell analysis reveals transcriptional heterogeneity of neural progenitors in human cortex, Nature Neuroscience 18 (5) (2015) 637–646. doi:10.1038/nn.3980.

[27] A. K. Shalek, R. Satija, X. Adiconis, R. S. Gertner, J. T. Gaublomme, R. Raychowdhury, S. Schwartz, N. Yosef, C. Malboeuf, D. Lu, J. J. Trombetta, D. Gennert, A. Gnirke, A. Goren, N. Hacohen, J. Z. Levin, H. Park, A. Regev, Single-cell transcriptomics reveals bimodality in expression and splicing in immune cells, Nature 498 (7453) (2013) 236–240. doi:10.1038/nature12172.

[28] D.-S. Lee, J.-Y. Shin, P. D. Tonge, M. C. Puri, S. Lee, H. Park, W.-C. Lee, S. M. I. Hussein, T. Bleazard, J.-Y. Yun, J. Kim, M. Li, N. Cloonan, D. Wood, J. L. Clancy, R. Mosbergen, J.-H. Yi, K.-S. Yang, H. Kim, H. Rhee, C. A. Wells, T. Preiss, S. M. Grimmond, I. M. Rogers, A. Nagy, J.-S. Seo, An epigenomic roadmap to induced pluripotency reveals DNA methylation as a reprogramming modulator., Nature communications 5 (2014) 5619. doi:10.1038/ncomms6619.

[29] H. Bagci, A. G. Fisher, DNA demethylation in pluripotency and reprogramming: the role of tet proteins and cell division., Cell stem cell 13 (3) (2013) 265 – 269. doi:10.1016/j.stem.2013.08.005.

[30] B. Zhang, H. Zheng, B. Huang, W. Li, Y. Xiang, X. Peng, J. Ming, X. Wu, Y. Zhang, Q. Xu, W. Liu, X. Kou, Y. Zhao, W. He, C. Li, B. Chen, Y. Li, Q. Wang, J. Ma, Q. Yin, K. Kee, A. Meng, S. Gao, F. Xu, J. Na, W. Xie, Allelic reprogramming of the histone modification H3K4me3 in early mammalian development., Nature 537 (7621) (2016) 553 – 557. doi:10.1038/nature19361.

[31] A. P. Feinberg, A. Levchenko, Epigenetics as a mediator of plasticity in cancer, Science 379 (6632) (2023) eaaw3835. doi:10.1126/science.aaw3835.

[32] D. Rossetto, N. Avvakumov, J. Côté, Histone phosphorylation: A chromatin modification involved in diverse nuclear events, Epigenetics 7 (10) (2012) 1098–1108. doi:10.4161/epi.21975.

[33] C. Plass, S. M. Pfister, A. M. Lindroth, O. Bogatyrova, R. Claus, P. Lichter, Mutations in regulators of the epigenome and their connections to global chromatin patterns in cancer, Nature Reviews Genetics 14 (11) (2013) 765–780. doi:10.1038/nrg3554.
URL `http://dx.doi.org/10.1038/nrg3554`

[34] A. V. Probst, E. Dunleavy, G. Almouzni, Epigenetic inheritance during the cell cycle, Nature Reviews Molecular Cell Biology 10 (3) (2009) 192–206. doi:10.1038/nrm2640.

[35] H. Easwaran, H.-C. Tsai, S. B. Baylin, Cancer epigenetics: tumor heterogeneity, plasticity of stem-like states, and drug resistance., Molecular Cell 54 (5) (2014) 716 – 727. doi:10.1016/j.molcel.2014.05.015.

[36] J. Lei, S. A. Levin, Q. Nie, Mathematical model of adult stem cell regeneration with cross-talk between genetic and epigenetic regulation, Proceedings of the National Academy of Sciences 111 (10) (2014) E880–E887. doi:10.1073/pnas.1324267111.
URL `http://www.pnas.org/lookup/doi/10.1073/pnas.1324267111`

[37] J. Lei, A general mathematical framework for understanding the behavior of heterogeneous stem cell regeneration, Journal of Theoretical Biology 492 (2020) 110196. arXiv:1903.11448, doi:10.1016/j.jtbi.2020.110196.
URL `https://doi.org/10.1016/j.jtbi.2020.110196`

[38] J. Lei, Evolutionary dynamics of cancer: From epigenetic regulation to cell population dynamics—mathematical model framework, applications, and open problems, Science China Mathematics 63 (3) (2020) 411–424. arXiv:1908.07048, doi:10.1007/s11425-019-1629-7.
URL `http://arxiv.org/abs/1908.07048` `http://link.springer.com/10.1007/s11425-019-1629-7`

[39] A. Moustakas, K. Pardali, A. Gaal, C.-H. Heldin, Mechanisms of TGF-β signaling in regulation of cell growth and differentiation, Immunol Lett 82 (1-2) (2002) 85–91.

[40] L. Yang, Y. Pang, H. L. Moses, TGF-β and immune cells: an important regulatory axis in the tumor microenvironment and progression, Trends Immunol 31 (6) (2010) 220–227.

[41] S. Bernard, J. Bélair, M. C. Mackey, Oscillations in cyclical neutropenia: New evidence based on mathematical modeling, Journal of Theoretical Biology 223 (3) (2003) 283–298. doi:10.1016/S0022-5193(03)00090-0.

[42] R. Huang, J. Lei, Dynamics of gene expression with positive feedback to histone modifications at bivalent domains, International Journal of Modern Physics B 32 (7) (2018) 1850075. doi:10.1142/S0217979218500753.
URL `https://www.worldscientific.com/doi/abs/10.1142/S0217979218500753`

[43] R. Huang, J. Lei, Cell-type switches induced by stochastic histone modification inheritance, Discrete & Continuous Dynamical Systems - B 24 (10) (2019) 5601–5619. doi:10.3934/dcdsb.2019074.
URL `http://aimsciences.org//article/doi/10.3934/dcdsb.2019074`

[44] C. Jopling, S. Boue, J. C. I. Belmonte, Dedifferentiation, transdifferentiation and reprogramming: three routes to regeneration., Nature Reviews Molecular Cell Biology 12 (2) (2011-02) 79 – 89. doi:10.1038/nrm3043.

[45] S. Collombet, C. Van Oevelen, J. L. S. Ortega, W. Abou-Jaoudé, B. Di Stefano, M. Thomas-Chollier, T. Graf, D. Thieffry, Logical modeling of lymphoid and myeloid cell specification and transdifferentiation, Proceedings of the National Academy of Sciences of the United States of America 114 (23) (2017) 5792–5799. doi:10.1073/pnas.1610622114.

[46] S. Thowfeequ, E.-J. Myatt, D. Tosh, Transdifferentiation in developmental biology, disease, and in therapy., Dev Dyn 236 (12) (2007) 3208–3217. doi:10.1002/dvdy.21336.